ELSEVIER

Materials Chemistry and Physics 53 (1998) 132–137

MATERIALS CHEMISTRY AND PHYSICS

Electrical characteristics of $(Pb,Sr)TiO_3$ positive temperature coefficient ceramics

Yuh-Yih Lu, Tseung-Yuen Tseng *

Department of Electronics Engineering and Institute of Electronics, National Chiao-Tung University, Hsinchu, Taiwan

Received 25 July 1997; received in revised form 24 November 1997; accepted 12 December 1997

Abstract

Electrical properties of the positive temperature coefficient of resistance (PTCR) ceramics of compositions $Pb_xSr_{0.994-x}Y_{0.006}TiO_3$ ($x=0.5$, 0.6 and 0.7) with Curie point over 140°C up to 280°C were studied. The built-in potentials formed at grain boundaries in these ceramics were determined on the basis of the Heywang model. These built-in potentials are found to increase with increasing temperature and contribute to the PTCR effect of the ceramics. The resistances of grain and grain boundary of the ceramics were studied using the complex-plane impedance method. It is clearly observed that the grain resistance of the ceramic is much smaller compared to its grain boundary resistance and the change in resistivity with temperature is contributed mainly by the variation of grain boundary resistance.

Keywords: Positive temperature coefficient of resistance; Heywang model; Built-in potentials; Complex-plane impedance method

1. Introduction

The positive temperature coefficient of resistance (PTCR) effect in donor doped polycrystalline $BaTiO_3$ was first discovered in 1955 [1]. The dramatical increase in the resistivity was observed near the Curie point T_C. The Curie point of doped semiconducting barium titanate PTCR ceramics can be shifted to a lower temperature range by the substitution of Sr^{2+} for Ba^{2+} and to a higher temperature range by the substitution of Pb^{2+} for Ba^{2+} [2]. As a consequence of these characteristics, the PTCR ceramics can be widely used in the automotive and appliance industries [3,4]. Owing to the marvellous developments in the application of PTCR ceramics, the PTCR effect has been, and still is, a very important research topic.

The most accepted model to explain the abrupt PTCR effect above T_C in barium titanate ceramics is the Heywang model [5]. He assumed a two-dimensional layer of acceptor states at grain boundary which results in a grain boundary barrier and attracts electrons from grain. Many authors have also contributed to the grain boundary PTCR theory using the complex-plane impedance method [6–8]. All the evidences that come from these studies reveal that the grain boundary resistance plays a dominant role in PTCR behavior. The mechanism of PTCR behavior is complicated. Daniels et al. [9] have reported that the barium vacancies formed at the grain boundaries performing acceptor contribute to the built-in potential. Al-Allak et al. [10] have mentioned that Mn acting as acceptors contribute to the built-in potential of the Mn-doped PTCR ceramics in the grain boundary region. Therefore, the built-in potential and acceptor states at grain boundary significantly influenced the PTCR effect of semiconducting barium titanate.

Other than barium titanate ceramics, the PTCR effect was also found in $(Pb,Sr)TiO_3$ ceramics [11–13]. There are few articles which investigate the grain boundary phenomena of $(Pb,Sr)TiO_3$ PTCR ceramics. The purpose of this work is to study electrical characteristics of the ceramics with the Curie point from 140°C to 280°C. Complex-plane impedance analysis was carried out at different temperatures around T_C to study the variation of grain boundary resistance with temperature.

2. Experimental

The samples with compositions of $Pb_xSr_{0.994-x}Y_{0.006}TiO_3$, where $x=0.5$ (LST50), 0.6 (LST60) and 0.7 (LST70), were prepared by the conventional solid-state reaction technique. PbO and TiO_2 were employed as the starting lead titanate powders. $SrCO_3$ was used to adjust the Curie point

* Corresponding author. Tel.: +886 3 5731879; fax: +886 3 5724361.

0254-0584/98/$19.00
PII S0254-0584(97)02073-7

to lower temperature. Y_2O_3 was added to make n-type semiconducting properties of lead titanate.

The mixtures of the raw materials were ball milled in deionized water for 24 h with plastic coated iron ball media in a plastic jar. The milled slurry was dried with the use of an oven and calcined at 900°C for 1 h. The calcined powders were then ball milled, dried again and ground to produce the starting semiconducting powders. The powders obtained were pressed into disks at a pressure of 600 psi. The disks were stacked inside an Al_2O_3 crucible packed with the same composition powders as the disks and covered with a tightly fitted lid to prevent volatilization of PbO during sintering. These disks were heated at a rate of 25°C min^{-1}, sintering performed at 1250°C for 1 h, cooled at 600°C h^{-1} to 600°C and thereafter at the natural cooling rate of the furnace to room temperature. The sintering procedure was conducted by a programmable sintering furnace (U-SUN Heating Co., LTD. Taipei, Taiwan).

An In–Ga alloy, used as electrodes, in the ratio 3:2 was painted on both sides of the sintered samples to form an ohmic contact. The d.c. resistivity–temperature characteristic was measured by using a two-probe method with a PA meter/d.c. voltage source (Hewlett-Packard, HP4140B). The complex-plane impedance data were obtained using an impedance analyzer (Hewlett-Packard, HP4192A) with zero bias voltage, and the amplitude of the a.c. signals was 1 V. The complex impedance was measured as a function of frequency (5 Hz to 13 M Hz) at various temperatures. Both d.c. and a.c. measurements were conducted in a programmable furnace which was heated at a rate of 3°C min^{-1} and held at the target temperature for enough time to ensure thermal equilibrium.

Resistivity was evaluated from the measured resistance multiplied by a geometrical factor A/t, where A and t are the area and thickness of the testing sample, respectively. The measured dielectric constant, ε_m, was calculated from the measured impedance (Z) with the following formula [14]:

$$\varepsilon_m = \frac{t\,\mathrm{Im}(1/Z)}{\omega \varepsilon_0 A} \tag{1}$$

where ω is the angular frequency and ε_0 is the permittivity of vacuum. A constant frequency of 10 KHz was used to measure ε_m.

3. Results and discussion

The measured d.c. resistivity versus temperature characteristics of the samples with different compositions are shown in Fig. 1. As indicated in this figure, the samples with various switching temperatures exhibit PTCR effect and this behavior is similar to that in $BaTiO_3$-based PTCR ceramics.

The mechanism of the PTCR effect in donor doped polycrystalline $BaTiO_3$ ceramics above T_C could be described appropriately by a grain boundary barrier model proposed by Heywang [5]. According to this model, a two-dimensional

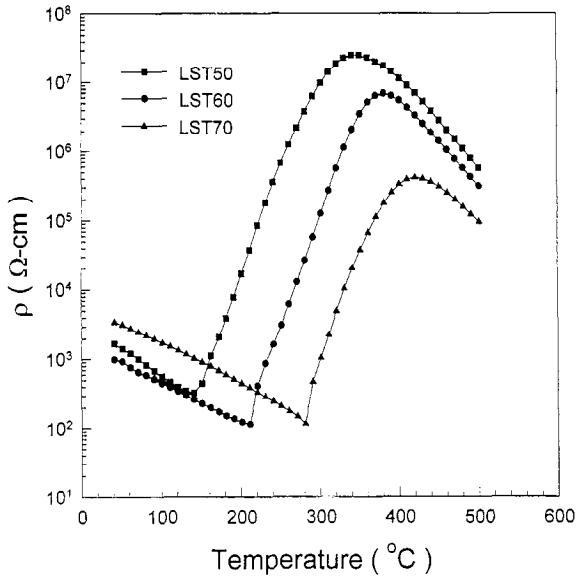

Fig. 1. Resistivity vs. temperature characteristics of the samples.

surface state with acceptor characteristics present at grain boundaries causes a built-in potential to reduce the probability of electrons passing through the grain boundaries. On the basis of this theory, the resistivity of the grain boundary is given by

$$\rho = \rho_o \exp\left(\frac{eV_{bi}}{KT}\right) \tag{2}$$

where ρ_o is constant, e is the unit electronic charge, K is the Boltzman constant, T is the absolute temperature and V_{bi} is the built-in potential at the grain boundaries which could be expressed as

$$V_{bi} = \frac{edN_e}{8\varepsilon_0 \varepsilon_m} \tag{3}$$

where N_e is the density of occupied acceptor states and d is the average grain size. Substituting Eq. (3) into Eq. (2), we obtain

$$\rho = \rho_o \exp\left(\frac{e^2 dN_e}{8\varepsilon_0 K \varepsilon_m T}\right) \tag{4}$$

According to Eq. (4), an Arrhenius plot of $\mathrm{Ln}(\rho)$ versus $(\varepsilon_m T)^{-1}$ would exhibit a linear relationship with a constant N_e. The average grain sizes were determined by a linear intercept method from the scanning electron microscopy (SEM) of the samples. By employing the data of ε_m (Fig. 2) and the average grain size, the density of occupied acceptor states can be calculated from the slope of the Arrhenius plot in the selected temperature region (Fig. 3). The insert diagram in Fig. 3 indicates that the calculated density of occupied acceptor states of the samples with various switching temperatures are found to decrease with increasing Pb content. Under the same fabrication process, the higher Pb content sample with lower N_e results in lower PTCR effect and higher T_{max}, which

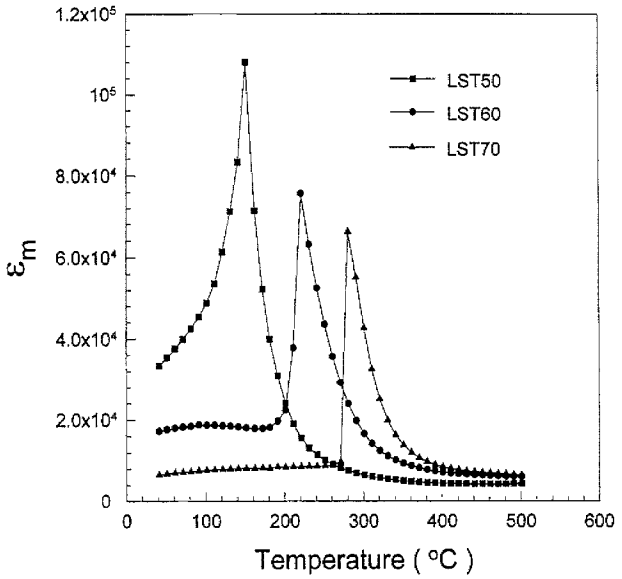

Fig. 2. The measured dielectric constant vs. temperature characteristics of the samples.

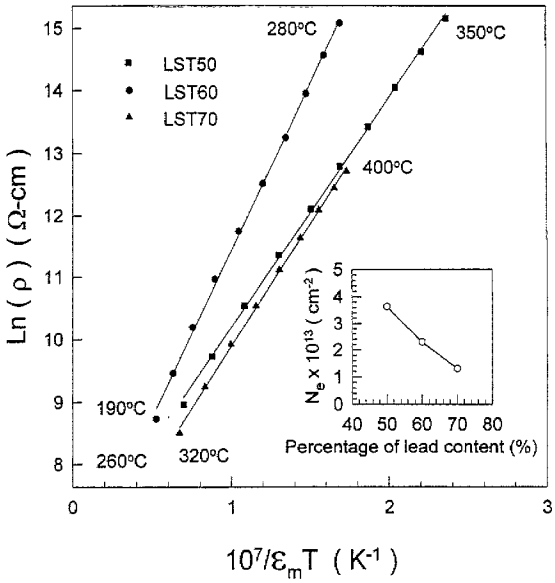

Fig. 3. Arrhenius plots of $(Pb,Sr)TiO_3$ ceramics. Temperature regions selected are also indicated. The insert shows the calculated N_e of the samples varied with Pb content.

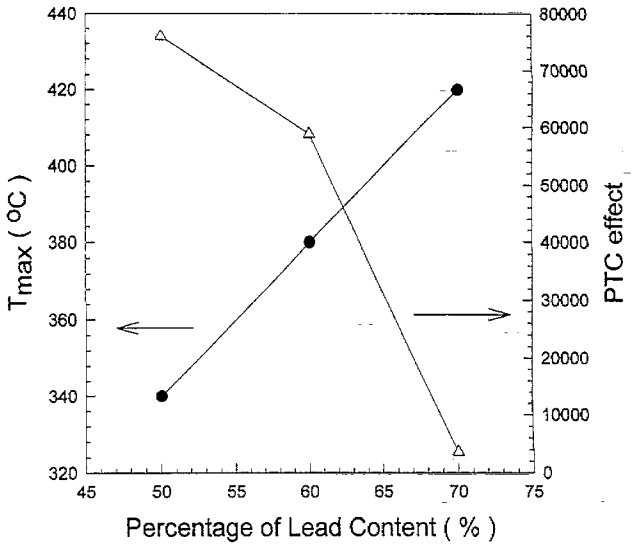

Fig. 4. Effect of lead content on the PTC effect and T_{max} of the samples.

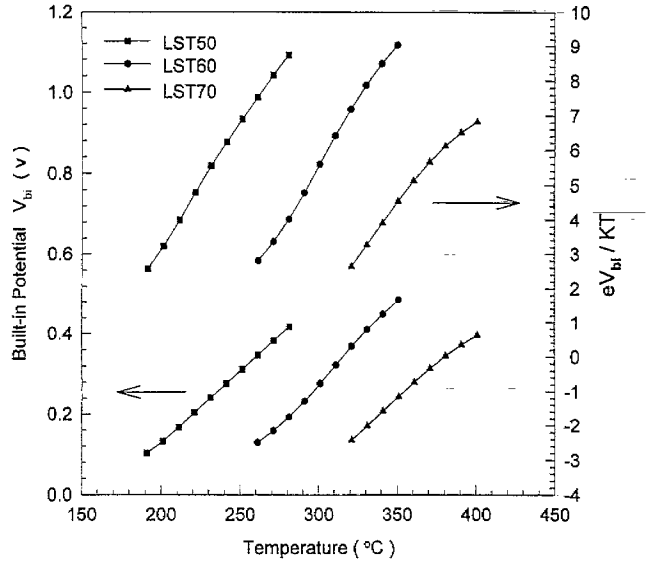

Fig. 5. Temperature dependance of calculated built-in potential and eV_{bi}/KT in PTCR region of $(Pb,Sr)TiO_3$ ceramics.

is the temperature at which the maximum resistivity appears (Fig. 4). This result agrees well with the observations of Al-Allak et al. [10] in $BaTiO_3$ PTCR ceramics. The built-in potentials of the samples can be obtained by knowing N_e on the basis of Eq. (3) and are shown as a function of temperature in Fig. 5, which indicates that the built-in potentials of the samples LST50, LST60 and LST70 increase with increasing temperature. According to Fig. 5 and Eq. (2), the increased built-in potential results in higher grain boundary resistance and is used to explain the PTCR effect for the samples.

The measured dielectric constant is related to the grain boundary layer permittivity [15,16] and can be expressed as

$$\varepsilon_m = \varepsilon_r \frac{dN_d}{N_e} \quad (5)$$

where N_d is the effective donor density per unit volume, ε_r the grain boundary permittivity. Within the temperature range in which N_e is constant, a plot of $1/\varepsilon_m$ versus temperature is expected to be linear if the grain boundary layer obeys the Curie–Weiss law. Fig. 6 shows $1/\varepsilon_m$ against temperature plots of the samples within the selected temperature region, in which a good linear relationship can be clearly observed for LST50, LST60 and LST70. This behavior indicates that the grain boundary layer permittivity obeys the Curie–Weiss law. The results discussed previously are in agreement with

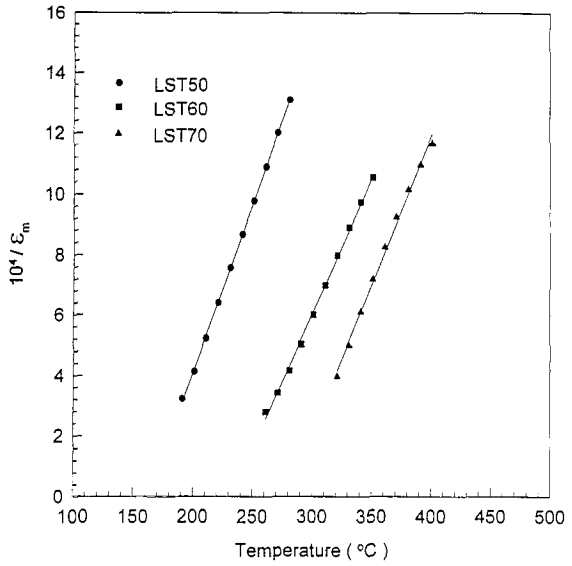

Fig. 6. Plots of $1/\varepsilon_m$ vs. temperature for the samples.

that observed in barium titanate ceramics [16]. Therefore, the Heywang model is suitable to be used to explain the grain boundary electrical properties of $(Pb,Sr)TiO_3$ PTCR ceramics.

The complex-plane impedance method is the most popular tool to characterize electrical properties of polycrystalline materials. The equivalent circuit shown in Fig. 7(a) is adopted as the electrical equivalent representation for the present samples, which a good ohmic contact forms at ceramic–electrode interfaces. The typical complex impedance diagram of this equivalent circuit, shown in Fig. 7(b), indicates that the part of the real axis intercepted by the arc is equal to grain boundary resistance, R_{gb}, the part of the real axis between the origin and the arc is equal to grain resistance, R_g [7]. In the present work we also used this popular technique to study the measured impedance data of our samples. The measured impedance can be expressed as

$$Z=\mathrm{Re}(Z)+j\mathrm{Im}(Z) \quad (6)$$

where $\mathrm{Re}(Z)$ and $\mathrm{Im}(Z)$ are the real and imaginary parts of the measured impedance, respectively. $-\mathrm{Im}(Z)$ is plotted as a function of $\mathrm{Re}(Z)$ to construct the complex impedance diagram. The measured complex impedance plots of the samples LST50, LST60 and LST70 with various applied frequencies under different testing temperatures are shown in Figs. 8, 9 and 10, respectively. From these figures, it is clear that one semicircular arc exists in the complex impedance diagram at a fixed temperature. This means that the In–Ga alloy forms a good ohmic contact and the equivalent circuit (Fig. 7) can be used to study the grain boundary resistances of the samples. It is also evident that the grain resistances of

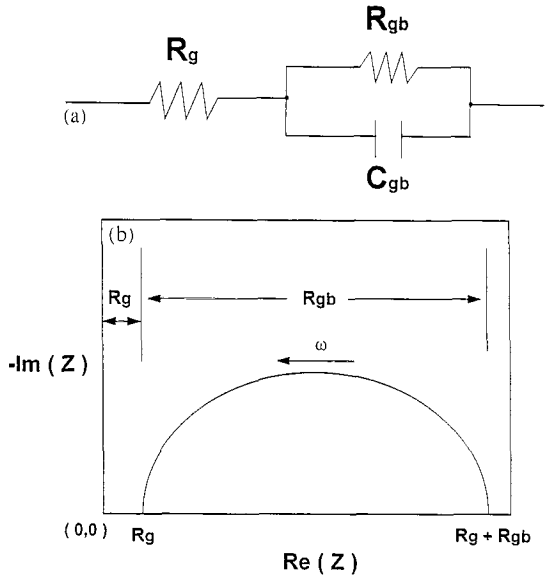

Fig. 7. (a) Equivalent circuit used for the samples. (b) Typical complex impedance diagram of circuit described in (a).

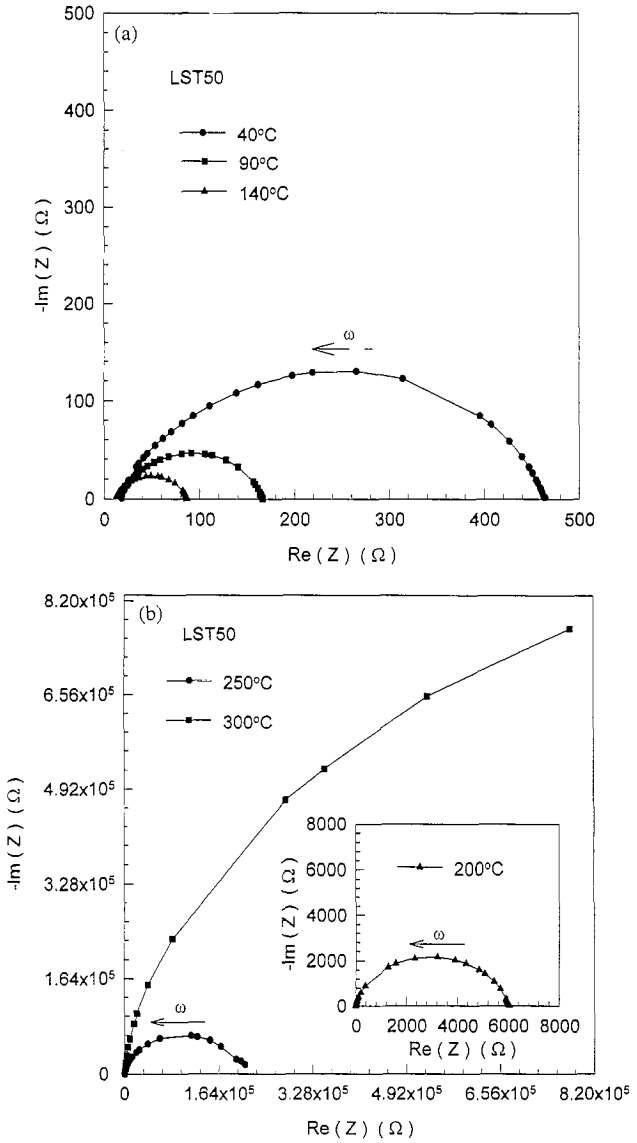

Fig. 8. Complex impedance plots for LST50 at six different temperatures: (a) 40°C, 90°C and 140°C; (b) 200°C, 250°C and 300°C.

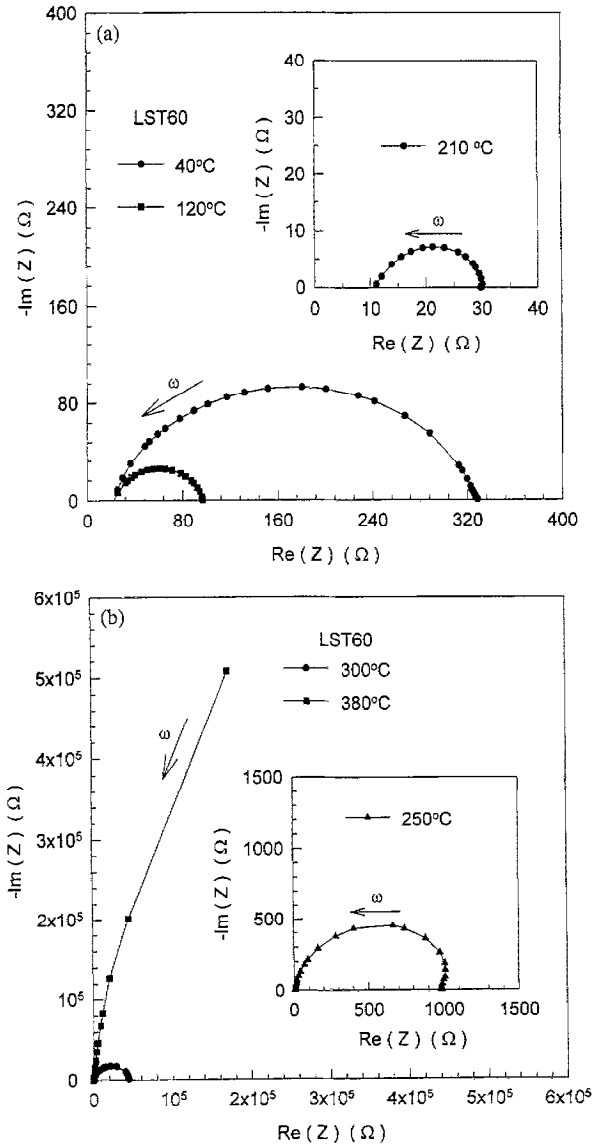

Fig. 9. Complex impedance plots for LST60 at six different temperatures: (a) 40°C, 120°C and 210°C; (b) 250°C, 300°C and 380°C.

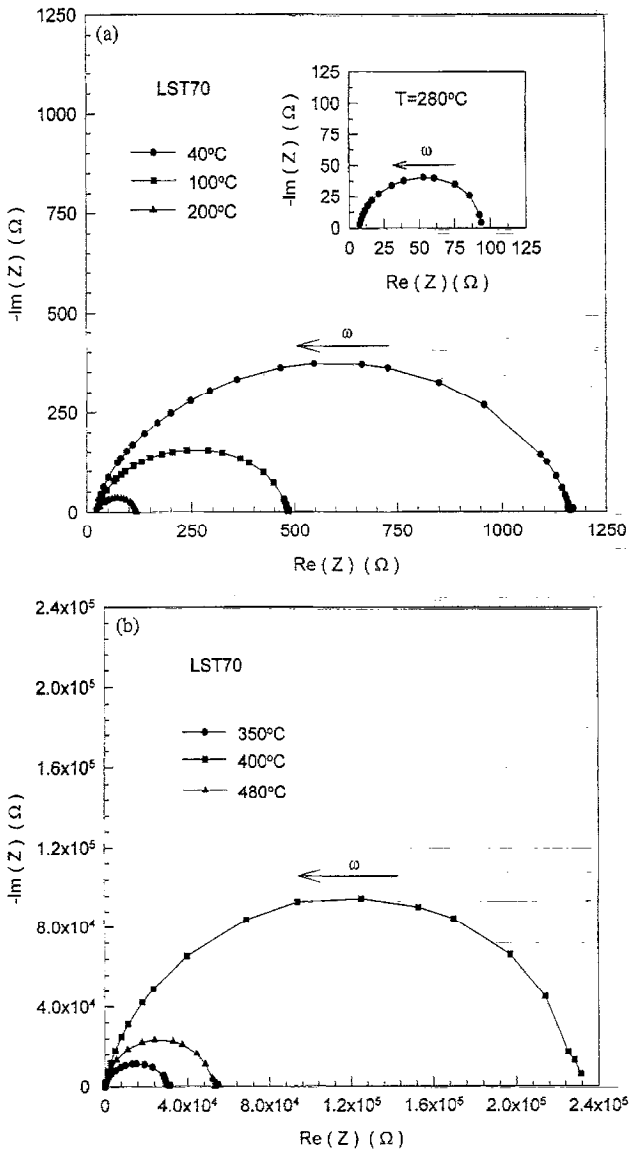

Fig. 10. Complex impedance plots for LST70 at seven different temperatures: (a) 40°C, 100°C, 200°C and 280°C; (b) 350°C, 400°C and 480°C.

the samples are varied slightly with various testing temperatures while the grain boundary resistances varied abruptly. From Figs. 8 and 9, the grain boundary resistances of LST50 and LST60 obtained from the real axis intercepted by the arc decrease with increasing temperature below T_C and increase with increasing temperature in the PTCR region. The grain boundary resistances significantly increase for LST50 and LST60 at 300°C and 380°C, respectively.

It can be seen in Fig. 10 that the grain boundary resistances of LST70 obtained from complex-plane impedance analysis increase with an increase in temperature in the PTCR region and decrease with an increase in temperature in the NTCR region. This phenomenon agrees with the result of the resistivity variation with temperature as shown in Fig. 1. On the basis of these observations, it is certain that the grain boundary resistance is the major contributor to the total resistivity of $(Pb,Sr)TiO_3$ ceramics.

4. Conclusions

Heywang's double Schottky model was adopted to investigate the grain boundary electrical characteristics of $(Pb,Sr)TiO_3$ ceramics. The abruptly increased d.c. resistivity in the PTCR region of the samples is due to the rising built-in potential. The decrease in the density of occupied acceptor states of the samples within the grain boundary layers with increasing Pb content results in lower PTCR effect and higher T_{max}. This phenomenon agrees with that observed in barium titanate PTCR ceramics. Plots of $1/\varepsilon_m$ against temperature for the samples in the selected temperature region reveal that

the grain boundary layer permittivity of the samples obeys the Curie–Weiss law. The changes in resistivity with temperature are primarily due to the variations of grain boundary resistance measured by the complex-plane impedance method. Therefore, it can be concluded that the temperature variation of resistivity of the samples is mainly due to the grain boundary resistive effect.

Acknowledgements

This work was supported by the National Science Council of the Republic of China under Project NSC 84-2215-E009-044.

References

[1] P.W. Haayman, R.W. Dam, H.A. Klassen, Ger. Patent No. 929350, June 1955.
[2] M. Kuwabara, J. Am. Ceram. Soc. 66 (11) (1983) c214.
[3] O. Saburi, K. Wakino, IEEE Trans. Compon. Parts CP-10 (1963) 53.
[4] A.L. Micheli, Ceram. Bull. 56 (1977) 783.
[5] W. Heywang, Solid State Electron. 3 (1961) 51.
[6] C.H. Lai, T.Y. Tseng, IEEE Trans. on CPMT, Part A 17 (2) (1994) 309.
[7] H.S. Maiti, R.N. Basu, Mater. Res. Bull. 21 (1986) 1107.
[8] D.C. Sinclair, A.R. West, J. Appl. Phys. 66 (1989) 3850.
[9] J. Daniels, K.H. Hardtl, R. Wernicke, Philips Tech. Rev. 38 (3) (1978–1979) 73.
[10] H.M. Al-Allak, A.W. Brinkman, G.J. Russell, J. Woods, J. Appl. Phys. 63 (9) (1988) 4530.
[11] Y. Hamata et al., Jpn. Patent No. 63-280401, Nov. 1988.
[12] C.K. Lee, I.N. Lin, C.T. Hu, J. Am. Ceram. Soc. 77 (5) (1994) 1340.
[13] Y.Y. Lu, T.Y. Tseng, IUMRS-ICEM Symp. Proc. 2 (1994) 69.
[14] C.H. Lai, T.Y. Tseng, J. Am. Ceram. Soc. 76 (3) (1993) 781.
[15] J. Illingsworth, H.M. Al-Allak, A.W. Brinkman, J. Phys. D: Appl. Phys. 23 (1990) 971.
[16] C.H. Lai, Y.Y. Lu, T.Y. Tseng, J. Appl. Phys. 74 (5) (1993) 3383.